Braun, M., Aranda-Ruiz, J., Rodríguez-Millán, M., Loya, J.A. (2018). On the bulk modulus and natural frequency of fullerene and nanotube carbon structures obtained with a beam based method, *Composite Structures*, v. 187, pp.: 10-17

.DOI: https://doi.org/10.1016/j.compstruct.2017.12.038

On the bulk modulus and natural frequency of fullerene and nanotube carbon structures obtained with a beam based method

M. Braun[b,c], J. Aranda-Ruiz[a,*], M. Rodríguez-Millán[a], J.A. Loya[a]

[a] Department of Continuum Mechanics and Structural Analysis, University Carlos III of Madrid, Avda. de la Universidad, 30. 28911 Leganés, Madrid, Spain
[b] Departamento de Construcciones, Facultad de Ingeniería, Universidad Nacional de La Plata, Avda. 1 esq. 47, La Plata B1900TAG, Argentina
[c] Consejo Nacional de Investigación Científicas y Técnicas (CONICET), CCT La Plata, Calle 8 N° 1467, La Plata B1904CMC, Argentina

ARTICLE INFO

Keywords:
Spherical fullerenes
Carbon nanotubes
Bulk modulus
Free vibrations
Finite element analysis
Beam based method

ABSTRACT

In this work, the natural frequency of vibration and Bulk modulus under hydrostatic pressure conditions of carbon nanotubes and fullerenes are investigated. For this purpose, three-dimensional finite element modelling is used in order to evaluate the vibration characteristics and radial stiffness for different nanotube and fullerene sizes. The atomistic method implemented in this work is based on the notion that nanotubes, or fullerenes, are geometrical frame-like structures where the primary bonds between two neighbouring atoms act like load-bearing beam members, whereas an individual atom acts as the joint of the related load-bearing system. The current numerical simulations results are compared with data reported by other authors, highlighting the greater simplicity and the lower computational cost of the model implemented in this work compared to other molecular dynamics models, maintaining accuracy in the results provided.

1. Introduction

In the last two decades, significant progress has been achieved in the area of nano-engineering. Exceptionally high Young's modulus, large aspect ratio and ultra-low density make carbon nanotubes (CNTs) and spherical fullerenes ideal candidates for reinforcement materials [1]. Besides, potential modern applications involve the use of systems that may consist of micro and nanostructures, for example micro- or nano-electromechanical devices (MEMS or NEMS) [2] as well as in bio-technology and biomedical fields [3,4], whose dynamic properties are essential for its correct functioning. For these reasons many experimental and theoretical works deal with the nanostructures reinforced composites [1,5–7] and many others studies analyse the dynamic properties of such nanostructures [8–15].

Regarding to the mechanical properties of these kind of structures, there are plenty of experimental and theoretical techniques for the characterization of the Young's modulus of carbon nanotubes which show a wide dispersion of results, as pointed out in the review by Rafiee and Moghadam [16], and are concerned on the axial properties of CNTs [17]. The mechanical properties of CNTs in the transverse direction are less studied. In the nanostructures reinforced composites, the interfacial (matrix-reinforcement) residual stresses and failure mechanism of the nanocomposites are highly related to the transverse mechanical properties [1]. Also, for the CNT-based gas sensors, nanogears and hydrogen containers, the deformation of the CNT in the transverse direction cannot be ignored, this being the key issue in the failure of these nano devices. Furthermore, when metal nanodroplets are capillarity absorbed by CNTs, the deformation of the latter in the radial direction can be very large [18]. Therefore, it is important to understand the transverse mechanical properties of these nanostructures.

In the specific case of spherical fullerenes, some researches study their characterization mainly focusing on the analysis of fullerene C_{60} [19–23] and to a lesser extent on other spherical carbon-molecules [24–26]. Generally, their prognosticated mechanical, chemical, thermal, electric and electronic properties have broadened their potential applications of fullerenes, ranging from bio-sensors, drug delivery, modern microelectronics, and bio-film resistant surfaces, to artificial molecular motors, non-bearings, mechanical reinforcement for membranes and polymer composites [27–30].

The theoretical approaches for the modelling of the CNTs and Fullerenes behavior can be divided into three main categories: the atomistic approach, the continuum approach and the nanoscale continuum approach [17].

Atomistic modelling comprises an *ab initio* approach [31] and molecular dynamics (MD) techniques. After this, other atomistic modelling methods, such as tight-binding molecular dynamics were developed.

Generally, *ab initio* methods give more accurate results than MD, but they are computationally expensive and only possible to use for a small

number of molecules. MD can be used in large systems and provide good predictions, but it is still limited owing to its being very time consuming, especially with long or multi-walled structures. In recent years, the atomistic approaches, due to their greater computational cost, have been gradually replaced by continuum approaches which are, at the moment, the most appropriate for effective computational simulations of large systems.

The basic assumption of the continuum mechanics-based approach consists in modelling a discrete structure as a continuum shell [9,10,32,33]. Arash and Wang [34] showed the advantages of the continuum theory applied to the modelling of shells and plates. However, the atomic characteristics of carbon nanotubes, such as chirality, are not taken into account in the continuous shell approach, and so their effects on the mechanical behavior of CNTs cannot be captured. Furthermore, whatever the type of the continuum modelling approach, the replacement of the whole CNT structure by a continuum element is not a completely satisfactory method to evaluate CNT properties.

The nanoscale continuum modelling consists in replacing the Carbon–Carbon (C–C) bond by a continuum element. The main approach in nanoscale continuum modelling consists in considering different elements, such as rods, trusses, springs and beams, well described in elasticity theory, to simulate these C–C bonds.

In 2003, Li and Chou [35] have presented the beam based method (BBM) for modeling the deformations of CNTs. The notion that CNTs are geometrical space-frame structures was fundamental to their approach, leading to a classical structural mechanics analysis. The authors used the stiffness matrix method to simulate the CNTs as space-frame structures. This approach has been applied in different works in order to calculate the elastic moduli in single walled (SWCNT) and multi-walled carbon nanotubes (MWCNT) [17,35–38]. However, the BBM developed by Li and Chou [35] was not applied to calculate the fundamental frequencies of vibration and the Bulk modulus of carbon nanotubes and fullerenes.

Nowadays, many studies from the literature analyse this kind of structures using analytical techniques [9,25,39] and molecular dynamics approaches [1,18], which entail high complexity. The major advantages of the BBM are the greater conceptual simplicity and the improved computational efficiency in the analysis of carbon nanostructures deformations [35]. Furthermore, the Beam Based Method is computationally less expensive than the Molecular Dynamics and other nonlinear models [17,37,38,40] but provides less information regarding the stress–strain distribution in the structure, mainly in problems where the structure is submitted to large deformations.

In this work, based on the Li and Chou's work [35], a three-dimensional finite element model of CNTs and spherical fullerenes is proposed to calculate the fundamental frequency of vibration and the Bulk modulus under hydrostatic pressure conditions. The paper is organized as follows: the atomic structure of fullerenes and CNTs is shortly described in the second section. The model and general methodology to calculate the Bulk modulus is described in section three. In section four the results obtained are presented and compared to studies presented by other authors. Finally, in section five the conclusions of the paper are drawn.

2. Atomic structures

In this section we present a description of the atomic structure of carbon nanotubes and fullerenes.

2.1. CNTs structure

The structure of a CNT is defined by the chiral vector and chiral angle, $\vec{C_h}$ and θ respectively. Fig. 1 presents the formation process of a CNT by cutting a graphite sheet along the dotted lines and rolling it so that the tip of the chiral vector touches its tail, being $\vec{T}$ the translational

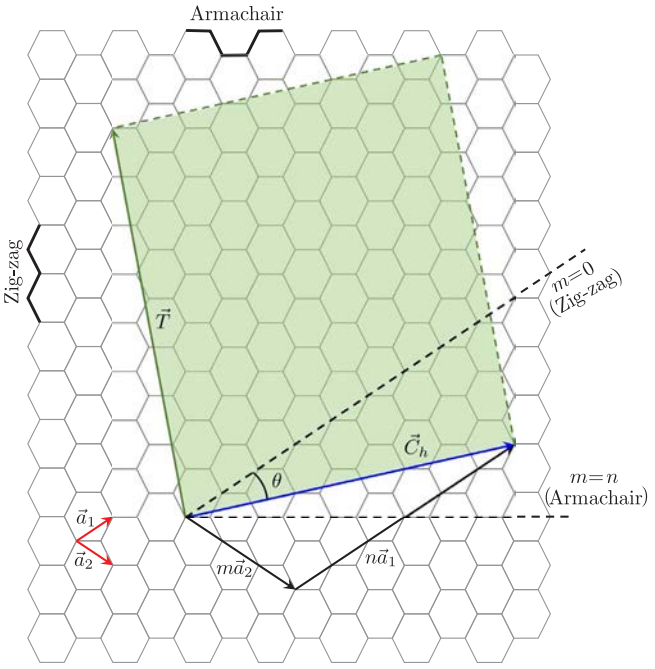

Fig. 1. Schematic illustration of an hexagonal graphene sheet with definition of chiral and translational vectors.

vector along the CNT axis. The chiral or roll-up vector, can be described as follows:

$$\vec{C_h} = n\vec{a_1} + m\vec{a_2}, \tag{1}$$

being the integers (n,m) the Hamada indices, and define the number of steps along the zigzag carbon bonds of the hexagonal lattice in the directions of the unit vectors $\vec{a_1}$ and $\vec{a_2}$ respectively.

The chiral angle θ is the angle between the chiral vector and the direction (n,0), and can be defined as [41]:

$$\theta = sin^{-1}\frac{\sqrt{3}\,m}{2\sqrt{n^2 + mn + m^2}}. \tag{2}$$

The chiral angle is limited for two cases, zigzag and armchair, being 0° and 30° respectively [42].

In terms of the roll-up vector, the zigzag nanotube is denoted by (n,0) and the armchair nanotube by (n,n). Fig. 2 shows the geometry of these kind of SWCNT.

The radius of any nanotube can be calculated as follows:

$$r_{NT} = \frac{a_0\sqrt{n^2 + mn + m^2}}{2\pi}, \tag{3}$$

where a_0 is defined as $a_0 = \sqrt{3}a_{C-C}$ with the equilibrium carbon–carbon (C–C) covalent bond length a_{C-C} usually taken to be 0.1421 nm.

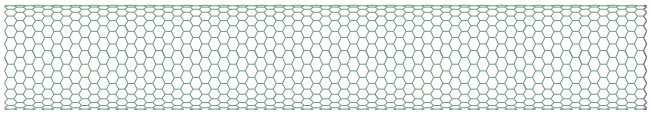

(a) Zigzag SWCNT

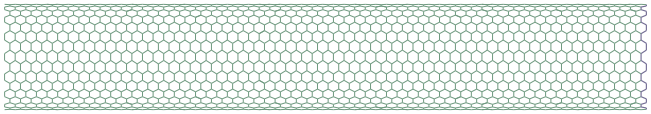

(b) Armchair SWCNT

Fig. 2. Configuration of the analyzed carbon nanotubes. (a) Zigzag SWCNT and (b) Armchair SWCNT.

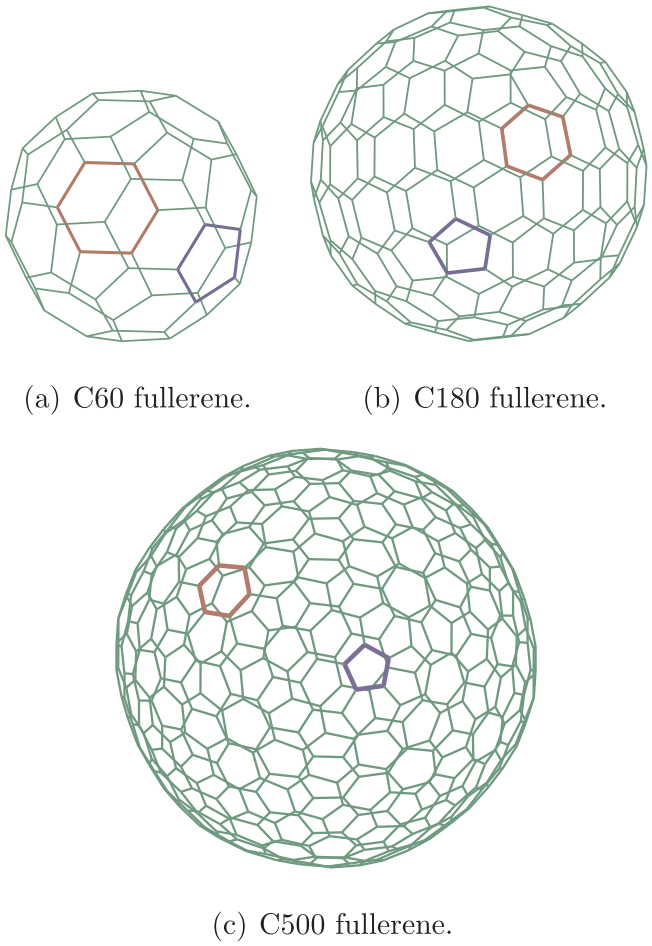

(a) C60 fullerene. (b) C180 fullerene.

(c) C500 fullerene.

Fig. 3. Configuration of some representative spherical fullerenes.

The physical properties of CNTs depends on their diameter, length and chirality. In particular, this last characteristic has a strong influence on the electronic properties of CNT [43]. The influence of chirality on the Bulk modulus of CNTs is analyzed in the present study for CNTs considered to be open without any fullerene end caps [32]. Regarding to the calculation of the fundamental frequency of vibration, only the armchair type has been considered, and the influence of the length and the diameter on this fundamental frequency has been analyzed.

2.2. Fullerenes structure

In this study, we consider fullerenes with spherical and non-spherical shape, and analyse different sizes C_i, where the number of carbon atoms i adopt the following values: 20, 30, 40, 50, 60, 70, 80, 90, 100, 180, 240, 260, 320, 500, 540, 720. Note that some molecules which may be synthesized in the future are modelled in the present work in order to clearly demonstrate the mechanical response variation for a wide range of fullerene sizes.

These structures are composed by a number of pentagons and hexagons depending on the number of carbon atoms that define them. Fig. 3 shows some representative sizes analyzed in this work.

The input atomic coordinates which define the topology of each molecule were initially taken from the fullerene library created by Yoshida [44].

3. FE model and general methodology

In the first part of this section, we describe in detail the Beam Based Method (BBM) implemented in this work. In the following parts, we explain the methodology used to calculate the Bulk modulus of CNTs and fullerenes, respectively.

3.1. Elastic constants of beam elements

The BBM was originally proposed by Odegard et al. [6], and developed by Li and Chou [35]. In this model, the elastic moduli of the beam elements are determined by establishing the link between inter atomic potential energies of the molecular structure and the strain energies of the equivalent continuum structure submitted to axial, bending and torsional deformations.

The force-field is expressed in the form of the total potential energy, which is uniquely defined by the relative positions of the nuclei composing the molecule. According to molecular dynamics, the total empirical inter-atomic potential energy of a molecular system is expressed as a sum of the individual energy terms due to bonded and non-bonded interactions [45]:

$$U = \sum U_r + \sum U_\theta + \sum U_\tau + \sum U_{vdw}, \tag{4}$$

where U_r stands for a bond stretch interaction, U_θ for a bond angle bending, U_τ for a bond torsion, and U_{vdw} for a non-bonded van der Waals interaction.

For covalent systems, the main contributions to the total potential energy comes from the first four terms of Eq. (4). Under the assumption of small deformations, the harmonic approximation is adequate for describing the energy [46]. By adopting the simplest harmonic forms and merging dihedral angle torsion and out-of-plane torsion into a single equivalent term, we get for each energy:

$$U_r = \frac{1}{2}k_r(r-r_0)^2 = \frac{1}{2}k_r(\Delta r)^2, \tag{5}$$

$$U_\theta = \frac{1}{2}k_\theta(\theta-\theta_0)^2 = \frac{1}{2}k_\theta(\Delta\theta)^2, \tag{6}$$

$$U_\tau = \frac{1}{2}k_\tau(\phi-\phi_0)^2 = \frac{1}{2}k_\tau(\Delta\phi)^2, \tag{7}$$

where k_r,k_θ and k_τ are the bond stretching force constant, bond angle bending force constant and torsional resistance respectively, while Δr,$\Delta\theta$ and $\Delta\phi$ represent bond stretching increment, bond angle variation and angle variation of bond twisting, respectively.

In order to determine the elastic moduli of beam elements, relations between the sectional stiffness parameters in structural mechanics and the force-field constants in molecular mechanics need to be obtained. The sections of the bonds are assumed to be identical and circular, and therefore the moments of inertia are equal. The elastic moduli that need to be determined are the Youngś modulus E and shear modulus G.

The deformation of a space-frame results in changes of strain energies. Thus, the elastic moduli can be determined through the equivalence of the energies due to the inter-atomic interactions and the energies due to deformation of the structural elements of the space-frame. As each of the energy terms of Eqs. (5)–(7) represents specific deformations, and no interactions are included, the strain energies of structural elements under specific deformations will be considered.

According to the theory of classical structural mechanics, the strain energy of a uniform beam of length L subjected to pure axial force N (see Fig. 4a) is

$$U_A = \frac{1}{2}\int_0^L \frac{N^2}{EA}\mathrm{d}L = \frac{1}{2}\frac{N^2L}{EA} = \frac{1}{2}\frac{EA}{L}(\Delta L)^2, \tag{8}$$

where ΔL is the axial stretching deformation. The strain energy of a

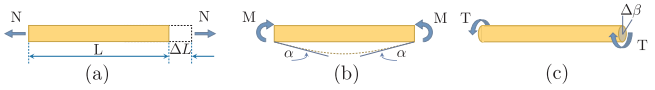

Fig. 4. Pure tension, bending and torsion of an element.

uniform beam under pure bending moment M (see Fig. 4b) is

$$U_M = \frac{1}{2}\int_0^L \frac{M^2}{EI}\mathrm{d}L = \frac{2EI}{L}\alpha^2 = \frac{1}{2}\frac{EI}{L}(\alpha)^2, \tag{9}$$

where α denotes the rotational angle at the ends of the beam. The strain energy of a uniform beam under pure torsion T (see Fig. 4c) is

$$U_T = \frac{1}{2}\int_0^L \frac{T^2}{GJ}\mathrm{d}L = \frac{1}{2}\frac{T^2L}{GJ} = \frac{1}{2}\frac{GJ}{L}(\Delta\beta)^2, \tag{10}$$

where $\Delta\beta$ is the relative rotation between the ends of the beam.

It can be seen that in Eqs. (5)–(10) both U_r and U_A represent the stretching energy, both U_θ and U_M represent the bending energy, and both U_τ and U_T represent the torsional energy. It is reasonable to assume that the rotation angle 2α is equivalent to the total change $\Delta\theta$ of the bond angle, ΔL is equivalent to Δr, and $\Delta\beta$ is equivalent to $\Delta\phi$. Therefore, by comparing Eqs. (5)–(7) with Eqs. (8)–(10), the following direct relationships between the structural mechanics parameters EA,IE and GJ and the molecular mechanics parameters k_r,k_θ and k_τ are obtained:

$$\frac{EA}{L} = k_r, \frac{EI}{L} = k_\theta, \frac{GJ}{L} = k_\tau. \tag{11}$$

Eq. (11) comprises the basis for the application of structural mechanics to the analysis of CNTs and carbon-related nano-structures. By assuming a circular beam section with diameter d, and setting $A = \pi d^2/4$,$I = \pi d^4/64$ and $J = \pi d^4/32$, Eq. (11) gives

$$d = 4\sqrt{\frac{k_\theta}{k_r}}, E = \frac{k_r^2 L}{4\pi k_\theta}, G = \frac{k_r^2 k_\tau L}{8\pi k_\theta^2}. \tag{12}$$

Eq. (12) establishes the foundations for applying the theory of structural mechanics to the modeling of carbon nanotubes or other similar fullerene structures. As long as the force constants k_r,k_θ and k_τ are known, the sectional stiffness parameters can be readily obtained. In this study, the bonds constants used are [47]: $k_r = 6.52 \times 10^{-7}$ N/nm, $k_\theta = 8.76 \times 10^{-10}$ Nnm/rad and $k_\tau = 2.78 \times 10^{-10}$ Nnm/rad and $L = 0.1421$ nm. The geometrical and material parameters are obtained from Eq. (12): $d = 0.147$ nm, $E = 5.49$ TPa and $G = 0.871$ TPa.

The three-dimensional finite element model is developed using the Abaqus/Standard commercial code. Bonds were modelled using 2 nodes linear beam elements with a single integration point (B31 elements in the Abaqus/Standard elements library). This uniaxial element presents tension, compression, torsion and bending capabilities, according with the BBM proposed by Li and Chou [35], and the works presented by other authors [17,37,38,40,48].

Initially, one beam element per bond was used in order to compare with the stiffness matrix method of Li and Chou [35]. However, the convergence tests carried out showed that if more elements are used, the results do not vary significantly. This is attributed to the fact that stretching is the major form of deformation of the beam element simulating the atomic bond.

The Finite Elements commercial code used in this work has implemented three different Eigensolvers, these are: Lanczos, Subspace and AMS. The values for the first natural frequency of vibration have been obtained using the three mentioned resolution methods, not observing differences between them.

The CPU time taken to solve the bulk modulus for a fully clamped (9,9) armchair CNT, and a Fullerene C60 are 38 and 30 s, respectively. For the same structures, the CPU time taken to calculate their natural frequencies are 40 s for the CNT and 48 s for the fullerene. As we can see, this approach has an acceptable CPU time to solve this type of problems.

3.2. Bulk modulus of CNTs

The Bulk modulus of the CNT is calculated according to its deformation under hydrostatic pressure P, following the same procedure presented in [18], by which the Bulk modulus is determined as the ratio of the pressure to the normalized volume change:

$$K = \frac{-P}{\Delta V/V_0}. \tag{13}$$

where V_0 is the initial volume of the CNT and ΔV is the mean volume decrease.

The volume V of a deformed CNT is calculated as:

$$V = \pi(r_{cnt} - \Delta r_{CNT})^2(l - \Delta l). \tag{14}$$

being r_{cnt} the radius of the carbon nanotube.

In this way, the relative volume change of a CNT under hydrostatic pressure is obtained as:

$$\frac{\Delta V}{V_0} = \left(1 - \frac{\Delta r_{cnt}}{r_{cnt}}\right)^2\left(1 - \frac{\Delta l}{l}\right) - 1. \tag{15}$$

where ΔV is the change of volume $V_0 - V$, and V_0 is the initial volume defined as $V_0 = \pi r_{cnt}^2 l$. The hydrostatic pressure is applied as a radial force f_r^i at each node i (with the help of a cylindrical coordinate system). This type of loading simulates the hydrostatic pressure P in the cylinder, which can be approximated by the following procedure:

$$P = \frac{\sum_{i=1}^{p} f_r^i}{2\pi r_{cnt} l}. \tag{16}$$

where p is the total number of carbon atoms in the nanotube.

3.3. Bulk modulus of Fullerenes

The Bulk modulus K of fullerenes is calculated using Eq. (13). In this case, the relative volume change of the spherical fullerene is related to the radial strain ε_r as follows:

$$\frac{\Delta V}{V_0} = 3\varepsilon_r. \tag{17}$$

considering tri-axial compression and small strains. At the same time, this radial strain is determined by:

$$\varepsilon_r = \frac{\Delta r_f}{r_f}. \tag{18}$$

where r_f is the initial radius of the fulleren and Δr_f is the mean radial displacement.

Also, a radial force f_r^i has been applied at each node i resorting to a spherical coordinate system, thereby simulating the hydrostatic pressure applied to the fullerene:

$$P = \frac{\sum_{i=1}^{p} f_r^i}{4\pi r_f^2}. \tag{19}$$

4. Results and discussion

In this section, we present the values of the Bulk modulus and first natural frequency of vibration, both for carbon nanotubes and fullerenes, obtained from numerical simulations. It is important to highlight that all the considered hydrostatic pressures are below the collapse limits, and consequently not instabilities are observed at all. Moreover, the BBM is valid only when small deformations have been taken into account, due to the fact that this method is not considering non-linearities, unlike other models as for example those based on Morse potential.

The computational results are compared with the limited existing theoretical results.

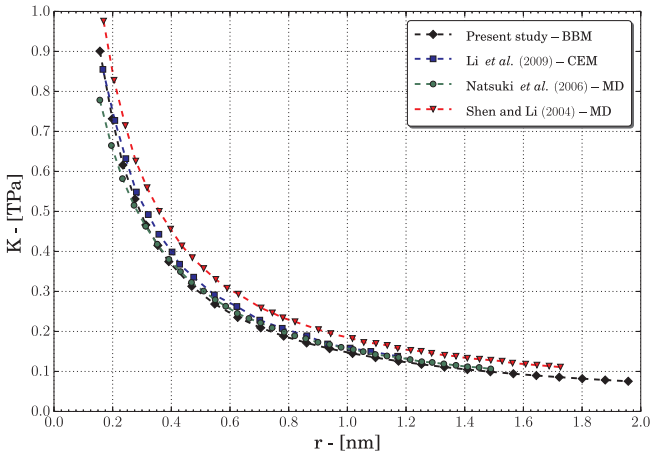

Fig. 5. Bulk Modulus as a function of zigzag CNT radius, predicted by different techniques.

4.1. CNTs bulk modulus

According to Eq. (13), the Bulk modulus of a zigzag CNT with different radius are plotted in Fig. 5. As we can see, the BBM results are in agreement with the results obtained using different techniques in the framework of Molecular Dynamics (MD) [49,50] and Continuum Elastic Method (CEM) [18].

All studies reveal the same trends, the Bulk modulus of carbon nanotube decreasing as the radius increases. The biggest difference is found with the work of Shen and Li [50], in which they propose an energy approach in the framework of molecular dynamics, about 22% for the nanotubes of grater radius and a 19% in an average value. The differences with the other two works, Natsuki et al. [49] and Li et al. [18], are considerably lower, 5% and 7% in an average difference value respectively. Natsuki et al. [49] use a molecular dynamics model coupled with atomistic-based continuum theory, which fits to the data obtained by our model, except for slight differences for smaller nanotube radius. Precisely in these smaller radius, is where our model best suits the one presented by Li et al. [18], who obtain the Bulk modulus using an analytical procedure based on the energy conservation, that is only valid for zigzag SWCNT with a small radius. It is important to note that the results provided by the model implemented in this paper (BBM) are between those provided by [50,49], which, despite being based on molecular dynamics models, differ greatly between them.

In the case of armchair SWCNT type, Fig. 6, reveals that the behaviour of the Bulk modulus is similar to the previous case, i.e. as the radius increases the Bulk modulus decreases. The differences with the results presented by other authors [50,49], are equivalent to those observed for the zigzag cases.

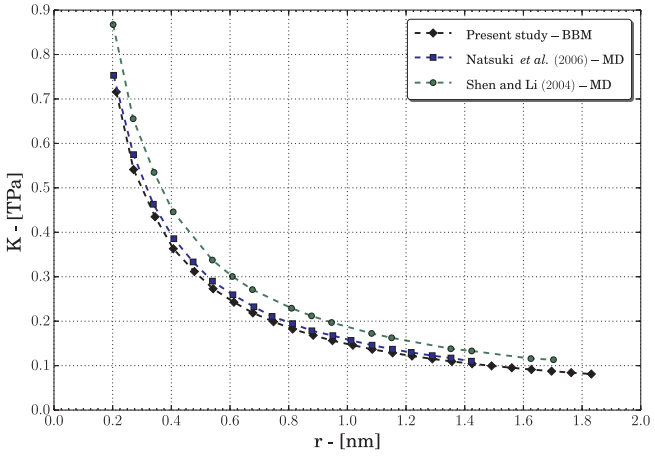

Fig. 6. Bulk Modulus as a function of armchair CNT radius, predicted by different techniques.

Table 1
Bulk modulus of fullerene C_{60} calculated by BBM and compared with results presented by other authors.

References	Method	K, TPa
Present work	BBM: beam based method	0.71
Tapia et al. [24]	SFEA: spring finite element analysis	0.83
Tapia et al. [24]	DFT: density functional theory	0.87
Giannopoulos et al. [26]	SBM: spring-based method	1.49
Kaur et al. [19]	TP: tersoff potential	0.67
Kaur et al. [19]	BP: brenner potential	0.69
Amer and Maguire [20]	MD: molecular dynamics	0.35
Woo et al. [21]	TBM: tight binding method	0.70
Ruoff and Ruoff [22]	BFM: bond force method	0.90
Ruoff and Ruoff [23]	CEM: continuum elasticity method	0.84

4.2. Fullerenes bulk modulus

In first place, the values of the Bulk modulus obtained by BBM for fullerene C_{60} is listed and compared with previous theoretical studies in Table 1.

If we compare each specific value of Bulk modulus presented in Table 1 with the corresponding average value of all of them (≃0.8 TPa), we can see that in all cases the error is lower than the 15% (specifically 12% for the model implemented in this work), except for the results presented by Giannopoulos et al. [26] and Amer and Maguire [20] where the error is 85% and 56%, respectively. In this way, it can be concluded that the model implemented in this work provides quite accurate results when compared to the average value of the results proposed by the rest of the authors.

The Bulk modulus value obtained in the current work shows a 26.76% difference with the results of the bond force method by Ruoff and Ruoff [22], due to the fact that this model only consider axial bond forces. Differences with the current Bulk modulus calculations are 16.90% for the Tapia et al. model [24] based on linear spring finite element analysis, and 109.86% for the spring-based method proposed by Giannopoulos et al. [26]. The use of the second spring element to simulate the bending interaction by Giannopoulos et al. explains the large difference observed. The model of Woo et al. [21] provides the smallest difference of 1.41%. The few discrepancies between the Bulk modulus results available in the literature and the results of the current study are due to different modelling approaches, potential functions, force fields constants, formulations for Bulk modulus determinations, etc.

Analyzing now the influence of fullerene size, Fig. 7 shows the Bulk modulus in function of fullerene radius obtained with different techniques: the spring-based method (SBM) [26], the spring finite element analysis (SFEA) [24], the density functional theory (DFT) [24] and the BBM implemented in this work. We can see that all the results exhibit the same tendency, where the Bulk modulus decreases as the radius increases. However, notable differences may be observed among different theoretical predictions of Bulk modulus for the same radius. Furthermore, we can see that the difference between theoretical predictions increases when the radius decreases.

Furthermore, the study presented by Giannopoulos et al. [26] is the only work that analyse all fullerene sizes. However, as stated before, the model implemented in [26] presents serious differences with respect to the Bulk modulus of the C_{60} obtained with other methods (≃85%). Therefore, in this work we present a complete calculus of the Bulk modulus for all spherical fullerene sizes, with a more accurate model.

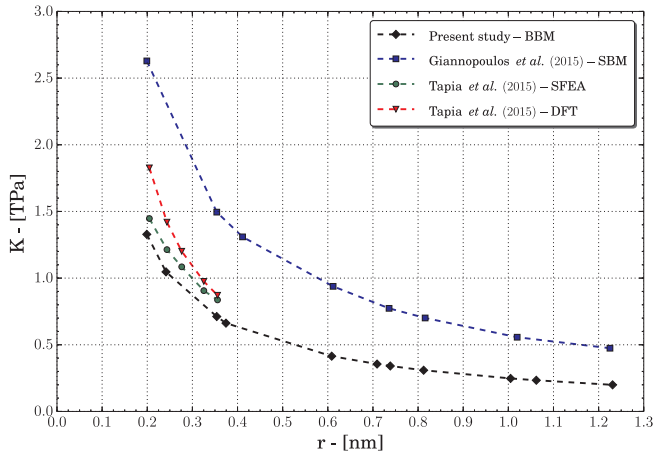

Fig. 7. Bulk modulus as a function of fullerene radius, predicted by different techniques.

4.3. CNTs fundamental frequency

The results obtained in the calculation of the natural vibration frequency of single walled carbon nanotubes (SWCNT) with the BBM have been compared with those presented by Ajori et al. [8], where a validated molecular dynamics code is used.

The geometry of nanotubes considered for the calculation of these vibration frequencies has been the arm-chair type (n,n), imposing also both ends clamped as boundary conditions (fully clamped).

In order to calculate these fundamental frequencies of vibration, the influence of both the length and the diameter of the carbon nanotube has been analyzed, according to what has been done in the work of Ajori et al. [8].

The results presented in Fig. 8 show the fundamental frequency of vibration for arm-chair SWCNT of 225.8 Å length. The effect of the width has been considered by varying the diameter of the *CNT* from 4.9 Å (corresponding to a (4,4) type) to 46.7 Å (corresponding to a (34,34) type).

It can be observed that as the diameter increases, the natural frequency of vibration decreases, a behavior properly reproduced by the BBM, according to the results presented in [8]. The difference between the results provided by both methods is only 7.5% in average value.

On the other hand, the Fig. 9 shows the value of the natural frequency of vibration as a function of the length of the nanotube. For this purpose, a nanotube of diameter 46.7 Å, corresponding to a geometry of the type (9,9) has been considered.

As in previous case, both methods provide very similar results. It can be observed that as the length increases, the natural frequency of vibration decreases. In this case, the difference between the results of both methods is about 12.6% in average value.

4.4. Fullerenes fundamental frequency

Regarding to the natural frequency of vibration for fullerenes, both spherical and ellipsoidal types of fullerenes have been considered, including a complete range of sizes. The spherical type include C_{60},C_{80},C_{180},C_{240},C_{320},C_{500} and C_{720} fullerenes. On the other hand, the non-spherical type are C_{20},C_{30},C_{40},C_{50},C_{70},C_{90},C_{100} and C_{540}.

The results obtained with the BBM have been compared with the presented by Adhikari and Chowdhury [51], who use a code of molecular dynamics. This comparison can be observed in Fig. 10.

Both methods show the same trend, since as the number of carbon atoms in fullerene increases (and thus their size), its fundamental vibration frequency decreases. The percentage difference between the results provided by both methods in this last case is about 20% in average value, slightly higher than in the case of nanotubes, but equally valid.

5. Conclusions

In this work, we have evaluated the capability of the implemented method to calculate the natural frequency of vibration and the Bulk modulus of carbon nanotubes and fullerenes. The obtained results are compared with data reported by other authors.

The Bulk modulus of the zigzag and armchair SWCNT decreases as the radius of the nanotube increases, with no significant differences between the zigzag and armchair configurations. These results are consistent with those presented by other authors, with which differences of 22% are obtained in the worst case.

Also, we observe that the Bulk modulus of fullerenes decreased when its size increases. In this way, the implemented model captures the same trend reported by other authors.

The Bulk modulus of the C_{60} obtained exhibit a good agreement with the values presented in the literature. The difference with the mean value reported results and our results is less than 12%. Hence, we have shown the capability of the model to predict the Bulk modulus in spherical fullerenes.

Regarding to the calculation of the natural frequency of vibration, it has been observed that the results provided by the BBM are in great agreement with those obtained by molecular dynamics codes, both in the nanotubes as in the fullerenes. The difference between the different methods is about 15% taking into account the results of carbon

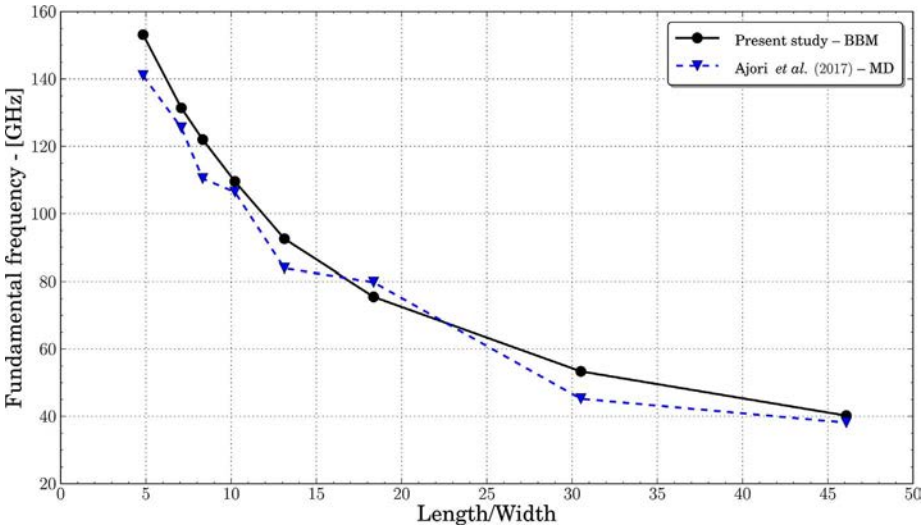

Fig. 8. Fundamental frequency of fully-clamped armchair SWCNT with different aspect ratios.

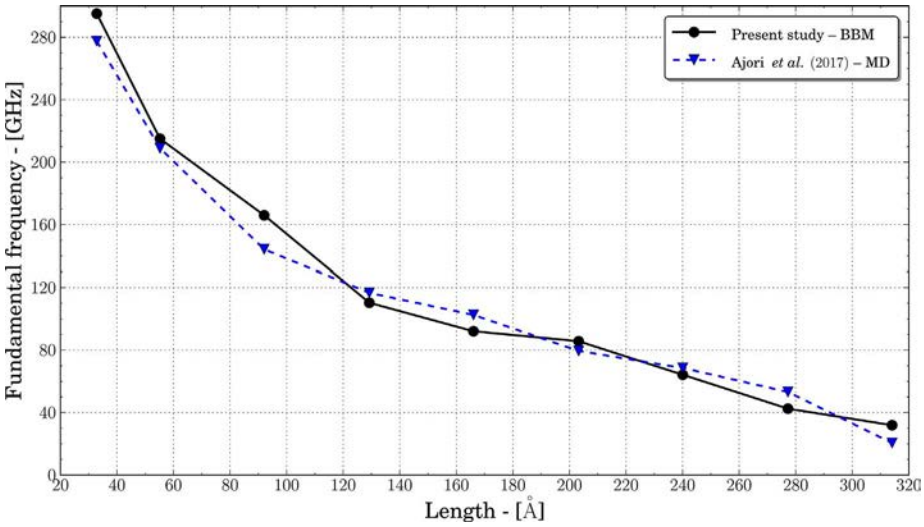

Fig. 9. Fundamental frequency of a fully-clamped (9,9) armchair SWCNT with different lengths.

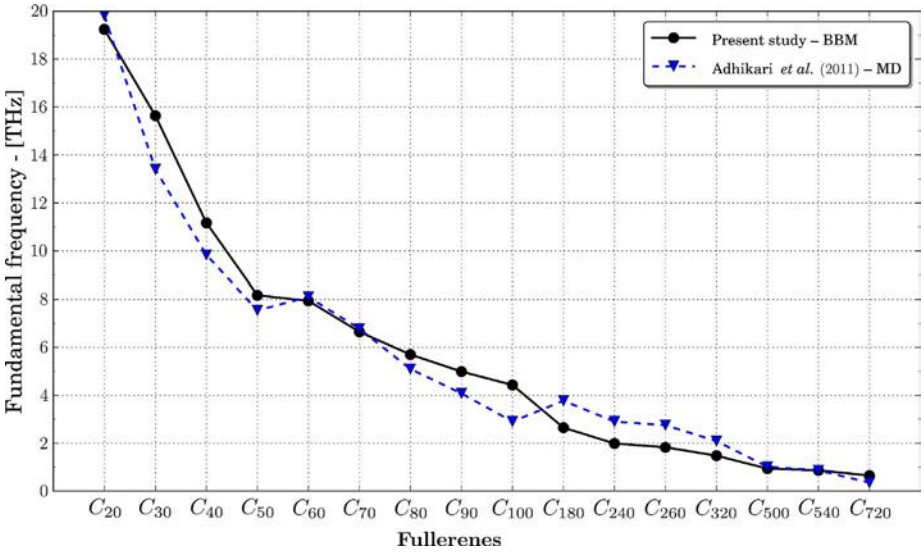

Fig. 10. Fundamental frequency of fullerenes family.

nanotubes and fullerenes.

The fundamental frequency of fully-clamped SWCNT decrease with its length (keeping the diameter constant) and with its diameter (keeping the length constant). Similarly, in the case of the fullerene family, the natural frequency decrease with the number of carbon atoms that conform the nanostructure.

Therefore, in this work we have presented a model capable of obtain accurately both the Bulk modulus as well as the natural frequency of vibration of carbon nanotubes and fullerenes. It is important to highlight the greater simplicity and the lower computational cost of the model implemented in this work compared to other molecular dynamics models, maintaining accuracy in the results and being one of the first works on providing the numerical results of the Bulk modulus of all spherical fullerenes sizes obtained with a more accurate model.

Acknowledgments

The authors are indebted to the Ministerio de Economía y Competitividad de España (Projects DPI2011-24068 and DPI2011-23191) for the financial support.

References

[1] Ajayan PM, Schadler LS, Giannaris C, Rubio A. Single-walled carbon nanotube-polymer composites: strength and weakness. Adv Mater 2000;12(10):750–3.
[2] Martin CR. Membrane-based synthesis of nanomaterials. Chem Mater 1996;8(8):1739–46.
[3] Kessentini S, Barchiesi D. Quantitaive comparison of optimized nanorods, nanoshells and hollow nanospheres for photothermal therapy. Biomed Opt Express 2012;3:590–604.
[4] Fazelzadeh S, Ghavanloo E. Coupled axisymmetric vibration of nonlocal fluid-filled closed spherical mambrane shell. Acta Mech 2012;223:2011–20.
[5] Wardle BL, Saito DS, García EJ, Hart AJ, de Villoria RG, Verploegen EA. Fabrication and characterization of ultrahigh-volume-fraction aligned carbon nanotube-polymer composites. Adv Mater 2008;20(14):2707–14.
[6] Odegard GM, Gates TS, Nicholson LM, Wise KE. Equivalent-continuum modeling of nano-structured materials. Compos Sci Technol 2002;62(14):1869–80.
[7] Lau AK-T, Hui D. The revolutionary creation of new advanced materials carbon nanotube composites. Compos Part B: Eng 2002;33(4):263–77.
[8] Ajori S, Ansari R, Haghighi S. Vibration characteristics of three-dimensional metallic carbon nanostructures with interlocking hexagons pattern (t6 and t14): a molecular dynamics study. Comput Mater Sci 2017;128:81–6.
[9] Loya J, Aranda-Ruiz J, Fernandez-Saez J. Torsion of cracked nanorods using a nonlocal elasticity model. J Phys D: Appl Phys 2014;47(11):115304.
[10] Aranda-Ruiz J, Loya J, Fernandez-Saez J. Bending vibrations of rotating nonuniform nanocamtilevers using the Eringen nonlocal elasticity theory. Compos Struct 2012;94(9):2990–3001.
[11] Lee JH, Lee BS, Au FTK, Zhang J, Zeng Y. Vibrational and dynamic analysis of c60 and c30 fullerenes using fem. Comput Mater Sci 2012;56:131–40.
[12] Narendar S, Gopalakrishnan S. Nonlocal wave propagation in rotating nanotube. Physics 2011;1:17–25.
[13] Pradhan SC, Murmu T. Application of nonlocal elasticity and DQM in the flapwise bending vibration of a rotating nanocantilever. Physica E 2010;42:1944–9.
[14] Murmu T, Adhikari S. Scale-dependent vibration analysis of prestressed carbon nanotubes undergoing rotation. J Appl Phys 2010;108:123507.

[15] Jing D, Pan Z. Molecular vibrational modes of c60 and c70 via finite element method. Eur J Mech A/Solids 2009;128:948–54.
[16] Rafiee R, Moghadam RM. On the modeling of carbon nanotubes: a critical review. Compos Part B: Eng 2014;56:435–49.
[17] Sakharova N, Pereira A, Antunes J, Brett C, Fernandes J. Mechanical characterization of single-walled carbon nanotubes: numerical simulation study. Compos Part B: Eng 2015;75:73–85.
[18] Li Y, Qiu X, Yin Y, Yang F, Fan Q. Equivalent elastic moduli of a zigzag single-walled carbon nanotube given by uniform radial deformation. Phys Lett A 2009;373(27–28):2368–73.
[19] Kaur N, Gupta S, Jindal V, Dharamvir K. Pressure induced transformations in condensed and molecular phases of c60. Carbon 2010;48(3):744–55.
[20] Amer MS, Maguire JF. On the compressibility of c60 individual molecules. Chem Phys Lett 2009;476(4–6):232–5.
[21] Woo S, Lee SH, Kim E, Lee K, Lee YH, Hwang SY, Jeon IC. Bulk modulus of the c60 molecule via the tight binding method. Phys Lett A 1992;162(6):501–5.
[22] Ruoff RS, Ruoff AL. The bulk modulus of c60 molecules and crystals: a molecular mechanics approach. Appl Phys Lett 1991;59(13):1553–5.
[23] Ruoff RS, Ruoff AL. Is c60 stiffer than diamond. Nature 1991;350:663–4.
[24] Tapia A, Villanueva C, Peón-Escalante R, Quintal R, Medina J, Peñunuri F, Avilés F. The bond force constant and bulk modulus of small fullerenes using density functional theory and finite element analysis. J. Mol. Model. 2015;21(139).
[25] Zaera R, Fernandez-Saez J, Loya J. Axisymmetric free vibration of closed thin spherical nano-shell. Compos Struct 2013;104:154–61.
[26] Giannopoulos GI, Georgantzinos SK, Kakavas PA, Anifantis NK. Radial stiffness and natural frequencies of fullerenes via a structural mechanics spring-based method. Fullerenes Nanotubes Carbon Nanostruct 2013;21(3):248–57.
[27] Chae S-R, Hotze EM, Wiesner MR. Possible applications of fullerene nanomaterials in water treatment and reuse. In: Sustich NSDDS, editor. Nanotechnology Applications for Clean Water, Micro and Nano Technologies. Boston: William Andrew Publishing; 2009. p. 167–77.
[28] Afreen S, Muthoosamy K, Manickam S, Hashim U. Functionalized fullerene (c60) as a potential nanomediator in the fabrication of highly sensitive biosensors. Biosens Bioelectron 2015;63:354–64.
[29] Ogasawara T, Ishida Y, Kasai T. Mechanical properties of carbon fiber/fullerene-dispersed epoxy composites. Compos Sci Technol 2009;69(11–12):2002–7.
[30] Kay E, Leigh D, Zerbetto F. Synthetic molecular motors and mechanical machines. Angew Chem Int Ed 2007;46(1–2):72–191.
[31] Kundin KN, Scuseria GE, Yakobson BI. C2F, BN, and c nanoshell elasticity from ab initio computations. Phys Rev B 2001;64:235406.
[32] Kalamkarov A, Georgiades A, Rokkam S, Veedu V, Ghasemi-Nejhad M. Analytical and numerical techniques to predict carbon nanotubes properties. Int J Solids Struct 2006;43(22–23):6832–54.
[33] Pantano A, Parks DM, Boyce MC. Mechanics of deformation of single- and multi-wall carbon nanotubes. J Mech Phys Solids 2004;52(4):789–821.
[34] Arash B, Wang Q. A review on the application of nonlocal elastic models in modeling of carbon nanotubes and graphenes. Comput Mater Sci 2012;51(1):303–13.
[35] Li C, Chou T-W. A structural mechanics approach for the analysis of carbon nanotubes. Int J Solids Struct 2003;40(10):2487–99.
[36] Li C, Chou T-W. Elastic moduli of multi-walled carbon nanotubes and the effect of van der waals forces. Compos Sci Technol 2003;63(11):1517–24.
[37] Tserpes K, Papanikos P. Finite element modeling of single-walled carbon nanotubes. Compos Part B: Eng 2005;36(5):468–77.
[38] Papanikos P, Nikolopoulos D, Tserpes K. Equivalent beams for carbon nanotubes. Comput Mater Sci 2008;43(2):345–52.
[39] Vila J, Zaera R, Fernandez-Saez J. Axisymmetric free vibration of closed thin spherical nanoshells with bending effects. J Vib Control 2016;22(18):3789–806.
[40] Meo M, Rossi M. Prediction of youngs modulus of single wall carbon nanotubes by molecular-mechanics based finite element modelling. Compos Sci Technol 2006;66(11–12):1597–605.
[41] Dresselhaus M. Carbon nanotubes. Carbon 1995;33(7):871–2.
[42] Rafii-Tabar H. Computational modelling of thermo-mechanical and transport properties of carbon nanotubes. Phys Rep 2004;390(4–5):235–452.
[43] Dresselhaus M, Dresselhaus G, Eklund P. Science of fullerenes and carbon nanotubes. San Diego: Academic Press; 1996.
[44] Yoshida M. Fullerene structure library, accessed in April 2015; 2015. URLhttp://jcrystal.com/steffenweber/gallery/Fullerenes/Fullerenes.html.
[45] Rappe AK, Casewit CJ, Colwell KS, Goddard WA, Skiff WM. UFF, a full periodic table force field for molecular mechanics and molecular dynamics simulations. J Am Chem Soc 1992;114(25):10024–35.
[46] Gelin B. Molecular modeling of polymer structures and properties. Cincinnati, HO: Hanser Gardner Publishers; 1994.
[47] Cornell WD, Cieplak P, Bayly CI, et al. A second generation force field for the simulation of proteins, nucleic acids, and organic molecules. J Am Chem Soc 1995;117(19):5179–97.
[48] Tserpes K, Papanikos P. The effect of stone-wales defect on the tensile behavior and fracture of single-walled carbon nanotubes. Compos Struct 2007;79(4):581–9.
[49] Natsuki T, Nayashi T, Endo M. Mechanical properties of single- and double-walled carbon nanotubes under hydrostatic pressure. Appl Phys A 2006;83:13–7.
[50] Shen L, Li J. Transversely isotropic elastic properties of single-walled carbon nanotubes. Phys Rev B 2004;69(4). 045414(10).
[51] Adhikari S, Chowdhury R. Vibration spectra of fullerene family. Phys Lett A 2011;375:2166–70.